

## Comparative Analysis of an integration of a Wind Energy Conversion System of PMSG and DFIG Models Connected to Power Grid

Sasi C.<sup>1</sup> and Dr. G. Mohan<sup>2</sup>

<sup>1,2</sup>*Department of Electrical Engineering,  
Annamalai University, Tamilnadu, India.  
E-mail: <sup>1</sup>saasi\_eeee@yahoo.co.in, <sup>2</sup>mg\_cdm@yahoo.com*

### Abstract

This paper presents the comparative analysis of an integration of a doubly fed induction generator and permanent magnet synchronous generator models fed to power grid. The large number of wind generators are going to be connected with the existing network in the near future. Therefore, it is necessary to analyse various models of wind energy conversion systems (WECS) for the purpose of studying the impacts upon grid. Both models are connected to AC grid through an efficient power electronic interface. Transient simulations are carried out under the condition of sudden short circuit disturbance and effect of increased generator inertia constant, friction factor and base speed is analysed. The power quality is also analysed in terms of total harmonic distortion for both models and steps are taken to improve the power quality by reducing total harmonic distortion.

**Keywords:** Permanent Magnet Synchronous Generator, Doubly Fed Induction generator, Power Electronic Interface, Power Quality, Total Harmonic Distortion.

### Nomenclature

THD	Total Harmonic Distortion
DFIG	Doubly Fed Induction Generator
WECS	Wind Energy Conversion System
EPEI	Efficient Power Electronic Interface
PMSG	Permanent Magnet Synchronous Generator
RSC	Rotor Side Converter
GSC	Grid Side Converter

$\omega_B$	Rotational speed of turbine
$P_w$	Power from the wind
$P$	Air density
$R$	Blade radius
$V_w$	Wind speed
$C_p$	Power coefficient
$\lambda$	Tip speed ratio
$\beta$	Blade pitch angle
$J$	Moment of inertia
$P_a$	Accelerate mechanical power
$u$	Voltage
$R$	Resistance
$i$	Current
$\omega$	Stator electrical frequency
$s$	Rotor slip
$L_s$	Stator leakage inductance
$L_r$	Rotor leakage inductance
$M$	Mutual inductance
$L_q, L_d$	q and d axis inductances

## Introduction

The development and utilisation of wind energy to satisfy the electrical demand has received considerable attention in recent years, owing to the concerns regarding the energy resources and enhanced public awareness of the potential impact of the conventional energy systems on the environment. Improvements in wind generation technologies will continue to encourage the use of wind energy in both the stand-alone and grid-connected systems [10], [9] & [7]. Owing to the random nature of the wind, the wind generators behave quite differently from the conventional generators. Therefore, it is important for the power system planners and engineers to carefully consider the reliability issues associated with the wind energy sources. A wind energy conversion system (WECS) converts the natural energy available at the system location into electrical energy. Directly interfacing the WECS to the utility gives rise to problems of voltage fluctuations, flickering and generation of sub-harmonics/harmonics [8],[2] & [5] associated with the pulsating torque, characteristic of the vertical axis wind turbine (prime mover) driving the induction generator. Hence, to overcome these difficulties generally, an asynchronous link is used to interconnect the WECS to the utility. The asynchronous link used in this paper

consists of rotor side converter (RSC), DC to DC intermediate circuit and grid side converter (GSC) as shown in Figure 1.

In terms of the generators for wind-power application, there are different concepts in use today. The major distinction among them is made between fixed speed and variable speed wind turbine generators. In the early stage of wind power development, fixed-speed wind turbines and induction generators were often used in wind farms. But the limitations of such generators, e.g., low efficiency and poor power quality, adversely influence their applications. With large-scale exploration and integration of wind sources, variable speed wind turbine generators, such as doubly fed induction generators (DFIG s) [6] & [1] and permanent magnetic synchronous generators (PMSGs) [3] & [4] are emerging as the preferred technology. In contrast to their fixed-speed counterparts, the variable speed generators allow operating wind turbines at the optimum tip-speed ratio and, hence at the optimum power efficient for a wide wind speed range.

In this paper, two different wind turbine generator systems (WTGS) models connected to AC grid through efficient power electronic interface capable of reducing total harmonic distortion (THD) noticeably during disturbances are proposed. The WECS model has a pitch-angled controlled, wind turbine, a generator model, a power system model with harmonic filters and power electronic interface having controlled converters. Simulations have been conducted with Matlab/ Simulink software to validate the model and the control schemes.

The generator speed is regulated to 1.09 p.u., reactive power to 0 p.u. and pitch angle to 0 degree. The two WTGS models are compared for increased generator inertia constant, increased generator friction factor and increased generator base speed. Further, power quality is analysed in terms of reducing THD using harmonic filters. Different types of symmetrical and asymmetrical faults are analysed under different wind generator power conditions with and without consider different harmonic filters at various bus locations of a power system.

## **Modeling of Wind Energy Conversion System with DFIG**

### **Model 1**

Half of the world's leading wind turbine manufacturers use the DFIG systems. Figure 1 shows a schematic of the WECS having WTGS Model 1 (DFIG) and efficient power electronic interface that will be discussed in this paper.

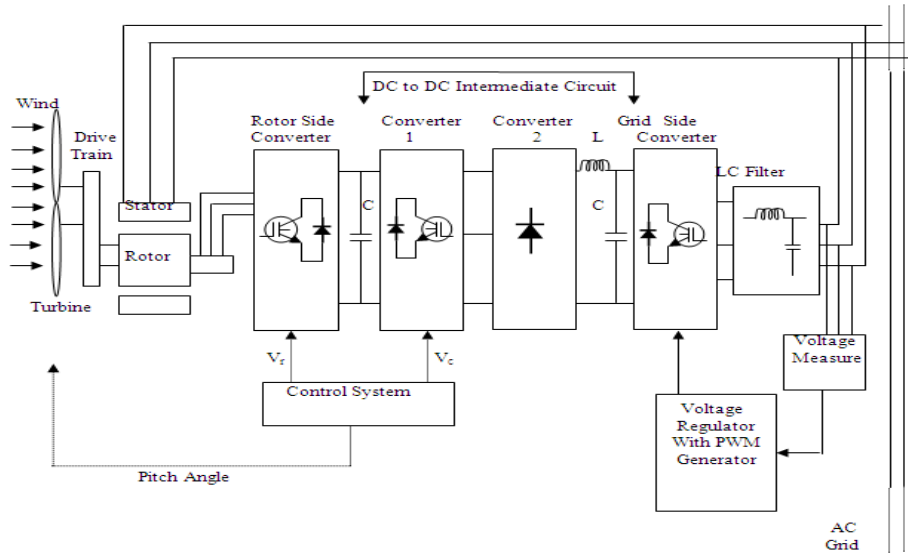


**Figure 1: Model 1: Wind Energy Conversion System with DFIG and Controlled Efficient Power Electronic Interface.**

The mechanical power available from a wind turbine

$$P_w = 0.5\rho\Pi R^2 V_\omega^3 C_p(\lambda, \beta) \quad (1)$$

$$C_p = \frac{1}{2} \times (\lambda - 0.022 \times \beta^2 - 5.6) \times e^{-0.17\lambda} \quad (2)$$

$$\lambda = \frac{V_\omega}{\omega_B} \quad (3)$$

where  $P_w$  is the extracted power from the wind,  $\rho$  is the air density,  $R$  is the blade radius and  $V_\omega$  is the wind speed.  $C_p$  is called the 'power coefficient' and is given as a nonlinear function of the parameters tip speed ratio  $\lambda$  and blade pitch angle  $\beta$ . The calculation of the performance coefficient requires the use of blade element theory.  $\omega_B$  is the rotational speed of turbine. Usually  $C_p$  is approximated as [14]-[15],

$$C_p = \alpha\lambda + \beta\lambda^2 + \gamma\lambda^3 \quad (4)$$

where  $\alpha$ ,  $\beta$  and  $\gamma$  are constructive parameters for a given turbine. The torque developed by the windmill is

$$T_t = 0.5\mu\left(\frac{C_p}{\lambda}\right) \cdot V_\omega^3 u R^2 \quad (5)$$

The equation of rotor motion is

$$\frac{d\omega_r}{dt} = \frac{2P_a}{J\omega_r} \quad (6)$$

where  $J$  is the moment of inertia due to the rotating mass and  $P_a$  is the rotor accelerate mechanical power. The angular velocity of the rotor is considered in the region  $0.7\omega \leq \omega_r \leq 1.3\omega$  for the case study presented in this paper.

The DFIG equations can be written as [16],

$$\frac{d\lambda_{ds}}{dt} = u_{ds} - R_s i_{ds} + \omega \lambda_{qs} \tag{7}$$

$$\frac{d\lambda_{qs}}{dt} = u_{qs} - R_s i_{qs} - \omega \lambda_{ds} \tag{8}$$

$$\frac{d\lambda_{dr}}{dt} = u_{dr} - R_s i_{dr} + s\omega \lambda_{qr} \tag{9}$$

$$\frac{d\lambda_{qr}}{dt} = u_{qr} - R_s i_{qr} - s\omega \lambda_{dr} \tag{10}$$

The stator electric values are indicated by the subscript s and the rotor electric values are indicated by the subscript r. u is a voltage, R is a resistance, i is a current, λ is a flux linkage. ω is the stator electrical frequency and s is the rotor slip. The flux linkages are given by

$$\lambda_{ds} = L_s i_{ds} + M i_{dr} \tag{11}$$

$$\lambda_{qs} = L_s i_{qs} + M i_{qr} \tag{12}$$

$$\lambda_{dr} = L_r i_{dr} + M i_{ds} \tag{13}$$

$$\lambda_{qr} = L_r i_{qr} + M i_{qs} \tag{14}$$

L<sub>s</sub>, L<sub>r</sub> and M are respectively the stator and the rotor leakage inductance and the mutual inductance between the stator and the rotor.

### Modeling of Wind Energy Conversion System with PMSG Model 2

The WECS considered here consists of WTGS having a PMSG driven by a wind turbine and efficient power electronic interface as shown in Figure 2. The modelling of wind turbine is same as that of Model 1. The dynamic model of PMSG is derived from the two-phase synchronous reference frame in which the q-axis is 90° ahead of the d-axis with respect to the direction of rotation. Figure 2 shows model 2 having PMSG and efficient power electronic interface.

The electrical model of PMSG in the synchronous reference frame is given as:

$$\frac{di_d}{dt} = \frac{v_d}{L_d} - \frac{Ri_d}{L_d} + \frac{L_q}{L_d} p\omega_r i_q \tag{15}$$

$$\frac{di_q}{dt} = \frac{v_q}{L_q} - \frac{Ri_q}{L_q} + \frac{L_d}{L_q} p\omega_r i_d - \frac{\lambda p\omega_r}{L_q} \tag{16}$$

$$T_e = 1.5p[\lambda i_q + L_{dq} i_d i_q] \tag{17}$$

where all quantities in the rotor reference frame are referred to the stator.

- L<sub>q</sub>, L<sub>d</sub> - q and d axis inductances
- R - resistance of the stator windings
- i<sub>q</sub>, i<sub>d</sub> - q and d axis currents
- v<sub>q</sub>, v<sub>d</sub> - q and d axis voltages
- ω<sub>r</sub> - angular velocity of the rotor
- λ - flux amplitude induced by the permanent magnets in the stator phases

$p$  - number of pole pairs  
 $T_e$  - electromagnetic torque.

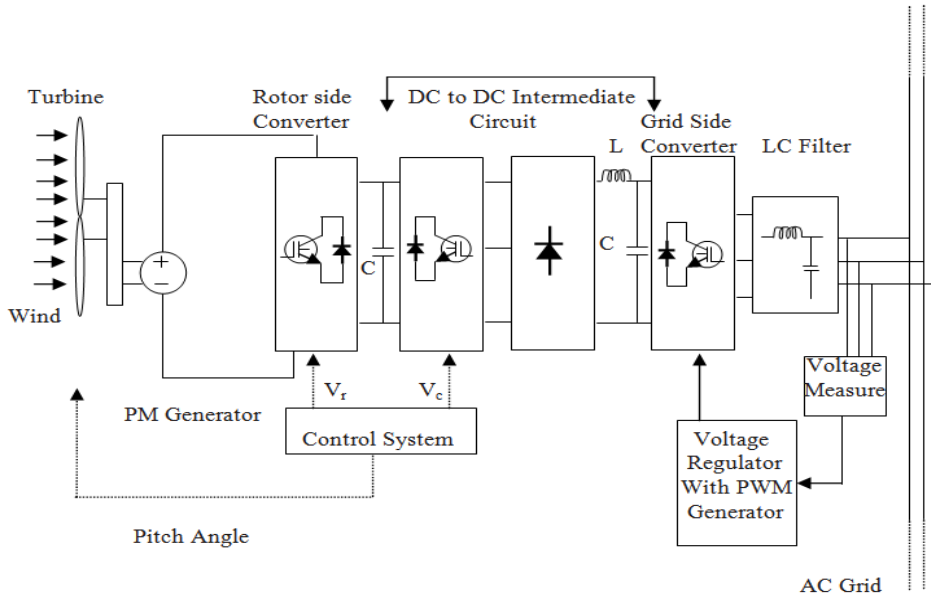


**Fig. 2. Model 2:** Wind Energy Conversion System with PMSG and Controlled Efficient Power Electronic Interface

The  $L_q$  and  $L_d$  inductances represent the relation between the phase inductance and the rotor position due to the saliency of the rotor. The inductance measured between phase  $a$  and  $b$  (phase  $c$  is left open)  $L_{ab}$  is given by:

$$L_{ab} = L_d + L_q + (L_q - L_d) \cos\left(2\theta_e + \frac{\Pi}{3}\right) \quad (18)$$

Where  $\theta_e$  represents the electrical angle. Mechanical system for the model is:

$$\frac{dw_r}{dr} = \frac{1}{J} (T_e - Fw_r - T_m) \quad (19)$$

$$\frac{d\theta}{dt} = w_r \quad (20)$$

where

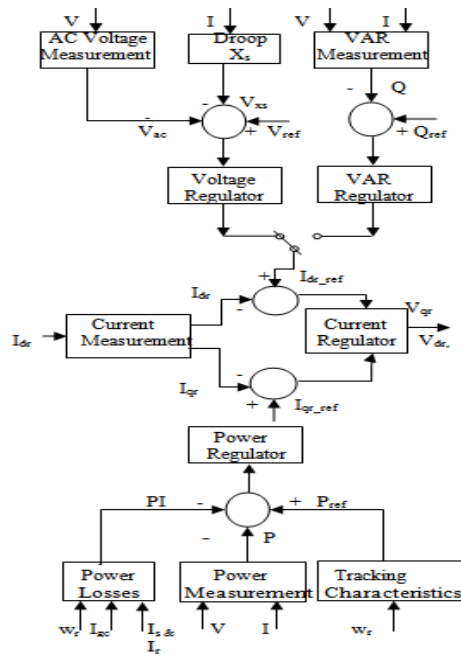
- $J$  Combined inertia of rotor and load.
- $F$  Combined viscous friction of rotor and load.
- $\theta$  Rotor angular position.
- $T_m$  SHAFT mechanical torque.

Table 1 shows the design parameters of DFIG and PMSG. Figure 3 shows voltage and VAR regulation of rotor side converter. The control system of converter 1

is illustrated in the Figure 4 and pitch control system is presented in the Figure 5. All the control systems shown in Figure 3 to 5 are used for both models.

**Table 1:** Generator parameters of Model 1 and Model 2.

Model 1	
Pnom (VA)	106 x 10 <sup>6</sup>
Rs (p.u)	0.0071
Ls (p.u)	0.1710
Rr (p.u)	0.0050
Lr (p.u)	0.1560
Lm (p.u)	2.9000
Model 2	
Pnom(VA)	2 x 10 <sup>6</sup>
Xd (p.u)	1.3050
Xd'' (p.u)	0.2520
Xq (p.u)	0.4740
Xq'' (p.u)	0.2430
Td'' (p.u)	0.0681
Tq'' (p.u)	0.0513
Rr (p.u)	0.0060



**Figure 3:** Voltage and VAR regulator of Rotor Side Converter.

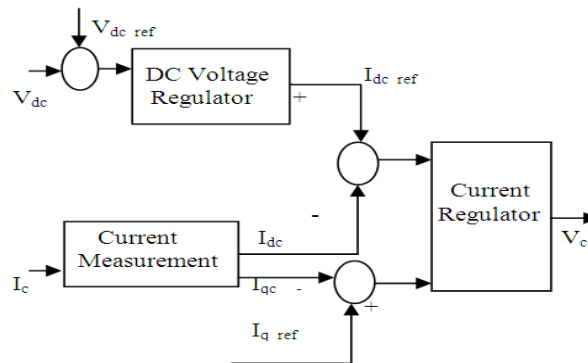


Figure 4: Voltage and Current regulator of Converter I.

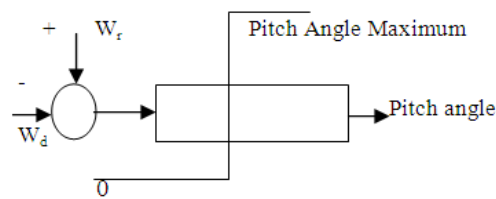


Figure 5: Pitch Angle control system.

**AC Power Grid with Harmonic Filters.**

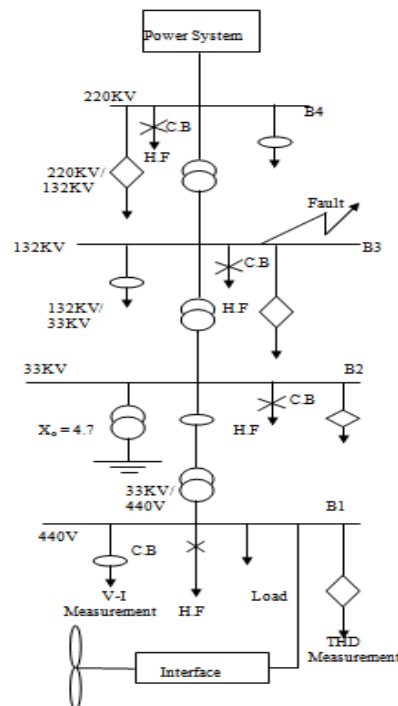


Figure 6: Power System Model.



**Power System Model**

The WECS having EPEI is connected to a 33 kV distribution system exports power to a 220 kV grid as shown in Figure 6. A-B fault at  $t=0.104$  s for a duration of 3 ms is simulated at B3. The wind speed is maintained constant at 10 m/s. The control system is used to maintain the speed at 1.09 pu and to regulate reactive power produced by the wind turbine at 0 MVAR.

Harmonic filters are included in power system model at bus B1 with a circuit breaker with transition time between 0.0667 and 0.1667 secs, breaker resistance of  $1 \times 10^2 \Omega$ , snubber resistance of  $1 \times 10^6 \Omega$  and snubber capacitance of infinite value.

**Three Phase Harmonic Filters**

Due to the significant amount of capacitance in a typical wind power plant, there is a high potential for resonance problems to occur [8], [9], [17]. That can result in unacceptable levels of harmonic current distortion at the substation capacitor banks, high voltage distortion at the MV bus of the plant main substation, and unacceptable harmonic current injected from the plant at the PCC. In order to reduce distortion, several banks of filters of different types are usually connected in parallel.

The filter set, used in paper, is made of the following four components:

- (i) One capacitor bank of 100 kVAR.
- (ii) Three filters.
  1. One C-type high-pass filter tuned to the 3rd harmonic (100 kVAR).
  2. One double-tuned filter 11th harmonic (100 kVAR).
  3. One high-pass filter tuned to the 24th harmonic (100 kVAR).

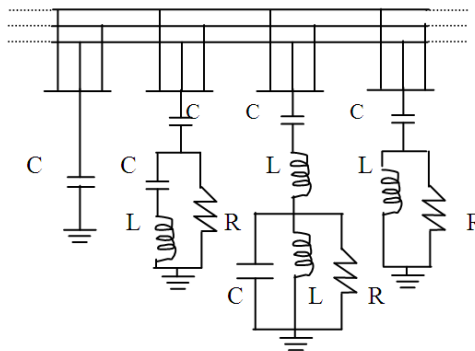


**Figure 7:** Three Phase Harmonic Filter set connected at various Busbar Location.

**Results and Discussion**

In this section the results obtained through simulations for the grid connection of the WECS using models 1 and 2 with efficient power electronic interface are presented.

**Effect of increased generator inertia constant**

As shown in Figure 8, with increase of inertia constant, generator speed regulation improves for model 1. The generator speed is required to be almost constant during fault. Hence, it is best regulated at 75% increase of inertia constant as increase in generator speed is less at 75%, while it is best regulated at no increase of inertia constant in case of model 2, as shown in Figure 9.

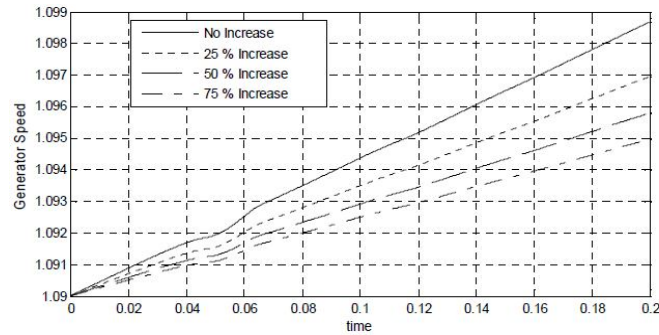


**Figure 8:** Effect of increased inertia constant on generator speed Model 1.

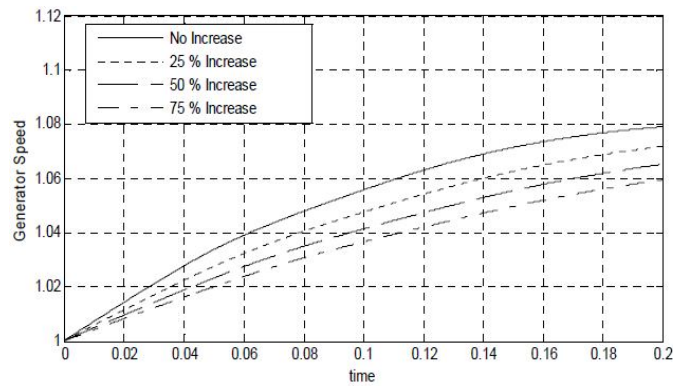


**Figure 9:** Effect of increased inertia constant on generator speed Model 2.

It is clear from Figure 10 that increases in inertia constant affects regulation of reactive power for model 1 during three phase fault. The maximum value of deviation from regulated value (0 p.u.) is 0.004, 0.0041, 0.0019 and 0.0042 for no increase, 25% increase, 50% increase and 75% increase respectively. Thus reactive power is best regulated at 50% increase of inertia constant for model 1. In case of model 2, the regulation of  $Q$  is best for 75% increase, as shown in Figure 11. The effect of increased inertia constant on reactive power is too less in case of model 1.

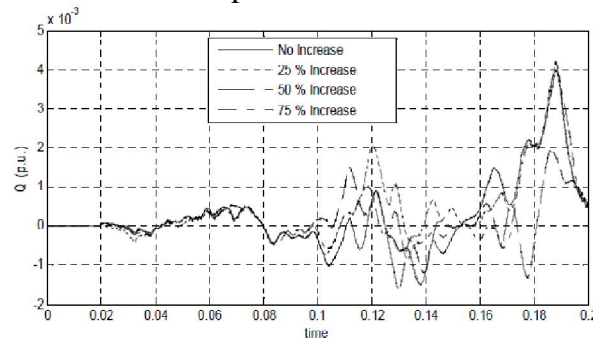


**Figure 10:** Effect of increased inertia constant on reactive power Model 1.

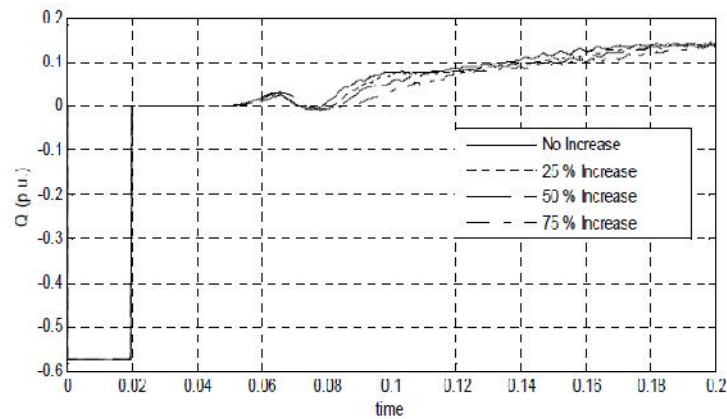


**Figure 11:** Effect of increased inertia constant on reactive power Model 2.

**Effect of increased generator friction constant**

It is seen that with increase of friction factor, regulation of generator speed becomes slightly better for model 1. As clear from Figure 12, the speed is best regulated at 75% increase of friction factor in case model 1. The speed regulation is best for no increase in model 2 as it is nearest to 1.09 p.u (as shown in Figure 13).

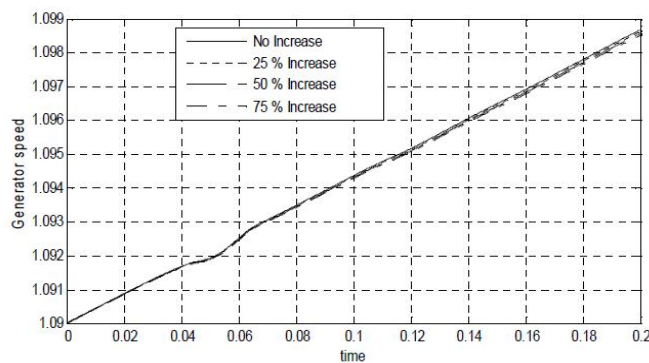


**Figure 12:** Effect of increased friction factor on generator speed (Model 1).

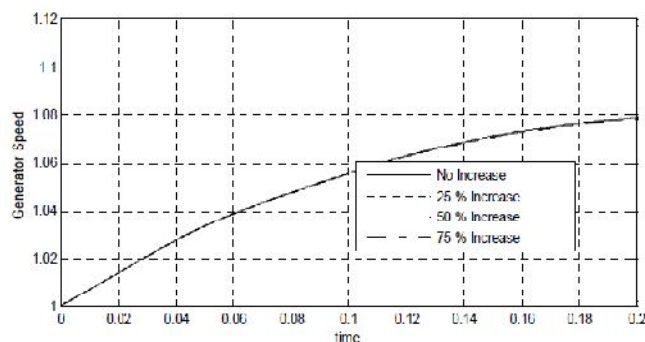


**Figure 13:** Effect of increased friction factor on generator speed Model 2.

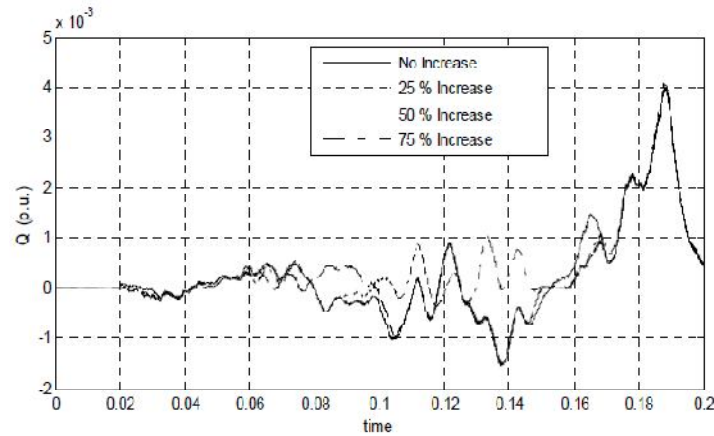


**Figure 14:** Effect of increased friction factor on reactive power (Model 1).

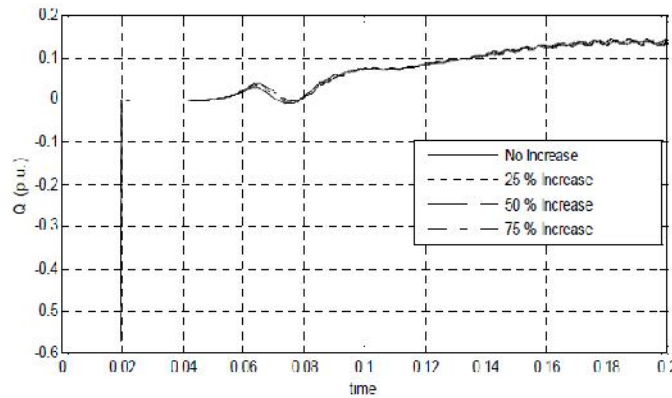


**Figure 15:** Effect of increased friction factor on reactive power Model 2.

### Effect of increased generator base speed

In model 1, the maximum deviation from regulated speed 1.09 p.u. is same for 50% increase and 75% increase, i.e., 0.0007, but for 50% increase the deviation is on positive side or generator speed increases and for 75% increase the deviation is on negative side or generator speed decreases as shown in Figure 16. Speed is best regulated for no increase of generator base speed in case model 2 as clear from Figure 17. It is shown in Figure 18 that  $Q$  is best regulated at 25% increase of base speed in case model 1. In case of model 2,  $Q$  is worst regulated for no increase while the curves are overlapping for 25%, 50% and 75% increase of generator base speed as in Figure 19. It is repeatedly seen that the effect of increased inertia constant on reactive power is too less in case of model 1.

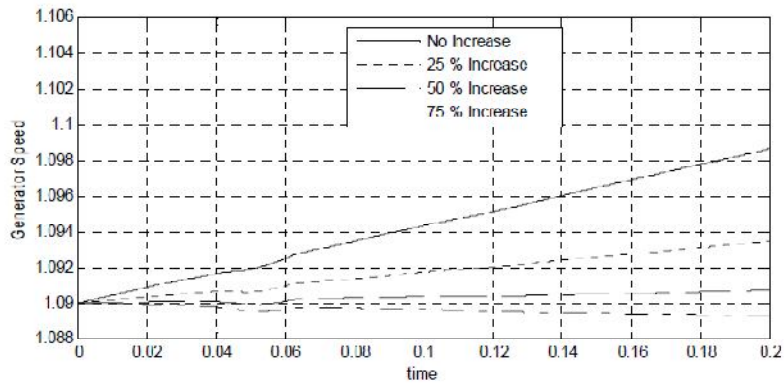


Figure 16: Effect of increased Generator base speed on generator Speed Model 1.

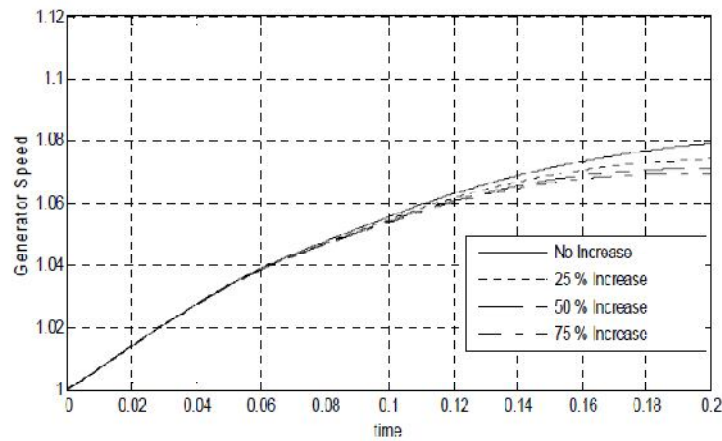


Figure 17: Effect of increased Generator base speed on generator Speed Model 2.

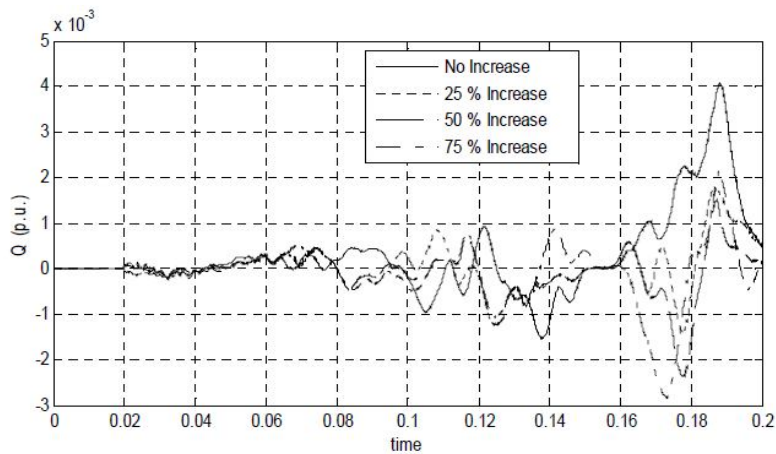
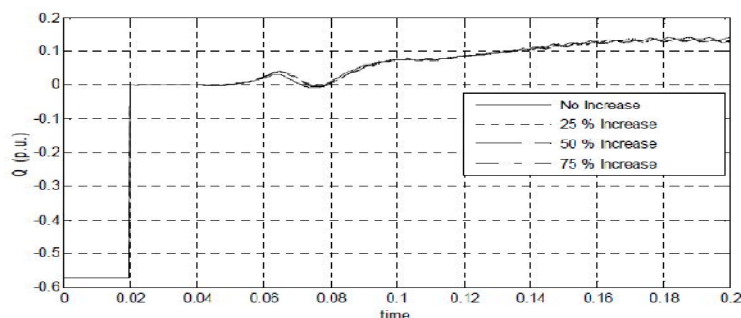


Figure 18: Effect of increased Generator base speed on reactive power Model 1.



**Figure 19:** Effect of increased Generator base speed on reactive power Model 2.

### Power quality analysis using harmonic filters

The effect of adding harmonic filters is analyzed using models 1 and 2 with three phase fault. The simulation results are shown briefly in Tables 2 and 3 for model 1.

Table 2 represents the effect of adding capacitor filter, then third harmonic filter, then 11/13<sup>th</sup> harmonic filter and lastly 24th harmonic filter at various locations (B1, B2, B3 and B4) in power system model. Table 3 presents the effect of adding harmonic filter set at different location of power system and effect of changing filter configurations and then again running simulations.

Here,

‘0’ - Represents decrease in THD

(in range 0.025–0.05);

‘00’- represents significant decrease in THD

(in range 0.05–0.075).

‘000’-represents more significant decrease in THD.

(more than 0.1).

‘x’ -represents increase in THD.

(less than 0.1).

‘xx’ Represents significant increase in THD.

(more than 0.1).

‘s’ - Represents approximately same.

Steps 2 to 4 are performed to decrease THD at various bus locations and increase power quality.

*Step 2:* Remove capacitor filter from B4 bus and run simulation. (S2).

*Step 3:* Remove capacitor filter from bus B3 and run simulation. (S3).

*Step 4:* Remove 24th harmonic filter from bus B4 and run simulation. (S4).

**Table 2:** THD measurements at various locations of power system by adding different harmonic filters, model 1.

THD Measurements							
1 <sup>st</sup>	3 <sup>st</sup>	11 <sup>st</sup>	24 <sup>st</sup>	1 <sup>st</sup>	3 <sup>st</sup>	11 <sup>st</sup>	24 <sup>st</sup>
Location: bus B1, Adding H.F.				Location: bus B2, Adding H.F.			
0	0	0	0	0	0	x	X
Location: bus B2, Adding H.F.				Location: bus B4, Adding H.F.			
0	0	0	0	0	0	x	X

**Table 3:** THD measurements by changing configuration of harmonic filter set, model 1.

THD Measurements								
Steps	B1	B2	B3	B4	B1	B2	B3	B4
	Bus B1, add H.F				Bus B2, add H.F			
S1	0	xx	000	0	0	xx	000	0
S2	0	xx	000	0	0	xx	000	0
S3	0	xx	000	0	0	xx	000	0
S4	0	xx	000	0	0	xx	000	0
Bus B3, add H.F				Bus B4, add H.F				
S1	0	0	000	0	0	s	x	x
S2	0	0	000	0	0	x	x	0
S3	0	0	000	0	0	s	x	0
S4	0	0	000	0	0	s	s	0

**Table 4:** THD measurements at various locations of power system by adding different harmonic filters, Model 2.

THD Measurements							
1 <sup>st</sup>	3 <sup>rd</sup>	11 <sup>th</sup>	24 <sup>th</sup>	1 <sup>st</sup>	3 <sup>rd</sup>	11 <sup>th</sup>	24 <sup>th</sup>
Location: bus B1, Adding H.F.				Location: bus B2, Adding H.F.			
0	0	0	x	0	0	x	x
Location: bus B3, Adding H.F.				Location: bus B4, Adding H.F.			
0	s	00	x	0	0	0	x

**Table 5:** THD measurements by changing configuration of harmonic filter set, model 2.

THD Measurements								
Steps	B1	B2	B3	B4	B1	B2	B3	B4
	Bus B1, add H.F				Bus B2, add H.F			
S1	0	xx	000	s	0	xx	000	0
S2	0	xx	000	s	0	xx	000	0
S3	0	xx	000	0	0	xx	000	0
Bus B3, add H.F				Bus B4, add H.F				
S1	0	0	000	0	0	s	x	x
S2	0	0	000	0	0	x	x	0
S3	0	0	000	0	0	s	x	0

Tables 4 and 5 present the simulation results briefly for model 2. Table 4 represents the effect of adding harmonic filters and Table 5 represents the effect of adding harmonic filter set at various bus locations of power system. Also, steps 2 and 3 are performed to reduce THD and hence enhance power quality.

*Step 2:* Active power from  $0$  to  $100 \times 10^6$ ; reactive power  $Q$  from  $50 \times 10^6$  to  $150 \times 10^6$ . (S2).

*Step 3:* Active power from  $100 \times 10^6$  to  $150 \times 10^6$ ; reactive power  $Q$  from  $150 \times 10^6$  to  $200 \times 10^6$ . (S3).

In step S3, the decrease in THD at B4 due to adding harmonic filter set at B4 is more significant than increase in THD at B4 due to adding harmonic filter set at B3.

## Conclusion

In this paper, grid connected WECS having two different WTGS models are compared during severe network disturbance. Power quality is also analysed and steps are taken to enhance it by reducing THD. A detailed model of the variable speed wind turbine with different generators connected to AC grid having harmonic filters through efficient power electronic interface is presented. At the same time, the paper addresses control schemes of the wind turbine in terms of pitch angle control, AC and DC voltage regulation, VAR regulation and current regulation of converter systems. The effect of increased generator parameters such as inertia constant, friction constant, base speed are examined for the above mentioned two types of WECS. Moreover, different types of symmetrical and asymmetrical faults are analysed at different power levels, with or without harmonic filters. Considering all the



simulation results, it can be concluded that the regarding efficient control of reactive power to 0 p.u. WECS having model 1 is effective and regarding control of generator speed to 1.09 p.u., WECS having model 2 is effective. The effect of changing generator parameters is less on generator speed and reactive power in case model 2. So, one can choose any model according to need of system. As a whole, it can be concluded that the proposed models can enhance the power quality of system during a transient fault and maintain the output reactive power at 0 p.u., rotor speed to 1.09 p.u., pitch angle to 0 degree and also reduces THD at various locations in power system.

## References

- [1] Beltran, B., Ahmed-Ali, T. and Benbouzid, M.E.H. (2008), "Sliding mode power control of variable-speed wind energy conversion systems", *IEEE Trans. on Energy Conv.*, Vol. 23, No. 2, pp.551–558.
- [2] Chang, G.W., Chen, C.I. and Teng, Y.F. (2010), "Radial-basis-function-based neural network for harmonic detection", *IEEE Trans. Ind. Electron*, Vol. 57, No. 6, pp.2171–2179.
- [3] Chen, J., Nayar, C.V. and Xu, L. (2000), "Design and finite-element analysis of an outer-rotor permanent-magnet generator for directly coupled wind turbines", *IEEE Trans. Magn.*, Vol. 36, No. 5, pp.3802–3809.
- [4] Huang, K., Zhang, Y., Huang, S., Lu, J., Gao, J. and Cai, L. (2009), "Some practical consideration of a 2MW direct-drive permanent-magnet wind-power generation system", *International Conference on Energy and Environment Technology*, 16–18 October, Guilin, China, Vol. 1, pp.824–828.
- [5] Lian, K.L. and Noda, T. (2010), "A time-domain harmonic power-flow algorithm for obtaining nonsinusoidal steady-state solutions", *IEEE Trans. Power Delivery*, Vol. 25, No. 99, pp.1–11.
- [6] Machmoum, M., Doeuff, R.L. and Sargos, F.M. (1992), "Steady state analysis of a doubly fed asynchronous machine supplied by a current controlled cycloconverter in the rotor", *Proc. Inst. Elect. Eng. B*, Vol. 139, No. 2, pp.114–122.
- [7] Nishikata, S. and Tatsuta, F. (2010), "A new interconnecting method for wind turbine/generators in a wind farm and basic performances of the integrated system", *IEEE Trans. Ind. Electron*, Vol. 57, No. 2, pp.468–475.
- [8] S.A. Papathanassiou and M.P. Papadopoulos, 2006, "Harmonic Analysis in a Power System with Wind Generation", *IEEE Transactions on Power Delivery*, Vol. 2, No.4, pp.2006–2016.
- [9] Ren, Z., Yin, Z. and Bao, W. (2009), "Control strategy and simulation of permanent magnet synchronous wind power generator", *International Conference on Energy and Environment Technology*, 16–18 October, Guilin, China, Vol. 1, pp.568–571.
- [10] Slootweg, J.G. and Kling, W.L. (2003), "Aggregated modeling of wind parks in power system dynamics simulation", *IEEE Power Tech. Conference*, Vol. 3, pp.1–6.

- [11] Slootweg, J.G., Polinder, H. and Kling, W.L. (2001), “Dynamic modelling of a wind turbine with doubly fed induction generator”, *Power Engineering Society Summer Meeting*, Vancouver, BC, Vol. 1, pp.644–649.